A New Voronoi-Based Blanket Coverage Control Method for Moving Sensor Networks

Farshid Abbasi, Afshin Mesbahi, and Javad Mohammadpour Velni

***Abstract*— This brief addresses the blanket coverage problem, in which it is desired to cover a long region by moving the blanket within the boundaries representing the main region. To this purpose, a group of autonomous mobile sensors are deployed aiming at maximizing the sensing performance. The blanket coverage area, which is considered to be a region with changing boundaries, is directed to move along the boundaries of the region. Throughout this process, the agents adapt to the varying coverage area by imposing the dynamics of the boundaries on their respective control law. The presented control law ensures that the agents move toward the centroid of their respective Voronoi cell while taking into account the effect of the moving boundaries. The proposed coverage method deploys the agents within the boundaries of coverage area and ensures the (locally) optimal partitioning for the moving coverage area. Performance of the proposed blanket coverage method is examined via numerical examples that use sections of Ohio river and a border buffer zone.**

***Index Terms*— Blanket coverage, coverage control, dynamic boundaries, multi-agent systems.**

I. Introduction

THERE have been advancements on developing techniques for deployment of a group of agents in a given environment to perform assigned distributed tasks [1], [2]. The core problem can be seen as a workload sharing task to assign the share of each agent from the total workload. The underlying optimization problem is NP-hard (nondeterministic polynomial-time hard) [3], and hence, finding a local minimum of the cost function is desired. The Voronoi partitions and Lloyd's algorithm are proposed as solutions to the coverage problem [4]. The existing methods in the literature can be employed to deploy agents in a given and invariant environment and may not address the case where, for various reasons, the coverage area changes dynamically.

Coverage control of areas, such as rivers and border buffer zones, is of great importance due to the environmental and geological significance of these areas. From the environmental point of view, rivers can be negatively impacted by various factors, including human activities, heavy metals, nitrogen, phosphorus, and acid mine [5], and monitoring of the quality of the surface water in rivers plays a critical role in conserving water resources [5], [6]. In addition, continuous access to regular information, such as recorded camera footage and measurement activities from border buffer zones, is required for surveillance and patrolling purposes [7]. To address the coverage problem in these areas or similar fields, several monitoring methods have been introduced, e.g., in [5] and [8] based on human activities or monitoring stations. However, the existing methods are not suitable to provide blanket coverage for real-time monitoring of a long section of such regions [9]. One reason is that these methods are not devised for time-varying coverage areas resulted from, e.g., dynamic boundaries. A coverage control method was recently proposed in [10] where multiple teams of agents operate, while the changing boundaries are taken into account in the formulation of the controller.

Recently, autonomous mobile sensor networks have been employed for real-time monitoring and data collection in rivers [11], [12] and other long regions and passages, such as border buffer zones [13]. In [14] and [15], an autonomous surface vehicle is used for measuring a range of water quality properties and greenhouse gas emissions while avoiding obstacles. Various aspects of patrolling and surveillance are studied in different application domains in [16], where the proposed methods can handle border patrolling while avoiding obstacles.

In several real-world applications, nonautonomous mobile sensor networks are employed to monitor long regions and passages while moving along the boundaries [17], [18]. In [19], a distributed coverage strategy is proposed based on square-grid blanket coverage for self-deployment of networked multirobot systems. Different motion coordination schemes are employed such as the nearest neighbor techniques that are based on clustering and autonomous coordination among sensor nodes in local area [20].

In this brief, we develop a new coverage control method for continuous and potentially long regions and passages. The objective is to move within boundaries to ensure the optimal coverage. It is noted that this brief investigates the design of a high-level controller, and hence, the dynamics of the agents and the characteristics of the underlying problems like flow dynamics in case of river-related applications are not taken into account. The motivation is to develop a generic control design method from blanket coverage perspective that has a plethora of applications in various fields. Therefore, depending on the application domain, the associated factors can be embedded in the problem formulation as an extension of this paper. For instance, in flow field applications, the properties of the flow, such as the velocity and the direction, can be captured. Therefore, it would be possible to improve reliability and energy consumption of the deployment algorithm by taking the low-level dynamics into consideration.

Manuscript received July 3, 2016; revised July 13, 2017; accepted September 23, 2017. Manuscript received in final form September 26, 2017. Recommended by Associate Editor Y. Shi. *(Corresponding author: Farshid Abbasi.)*

The authors are with the College of Engineering, The University of Georgia, Athens, GA 30602 USA (e-mail: javadm@uga.edu).

Color versions of one or more of the figures in this paper are available online at http://ieeexplore.ieee.org.

Digital Object Identifier 10.1109/TCST.2017.2758344

Throughout this brief, the boundaries of the region are modeled by two curves indicating the boundaries of the border buffer zones or rivers. Our objective is to cover the area by deploying agents that move within the boundaries of the region and converge to an optimum configuration within their respective coverage area. Therefore, the agents would be able to change (expand or compress) their area according to their missions, e.g., more accurate monitoring of certain parts of the region. The speed of the (moving) blanket coverage region and that of the boundaries determines the collective speed of the agents within their region. Two virtual guidance points are introduced to control the dynamics of the moving coverage region. The imposed dynamics on the guidance points affect the boundaries of the associated moving coverage region that in turn changes the dynamics of the agents. These guidance points are located in the rear and front areas of the moving region and determine the boundaries of the group of agents while moving along the main region. As an immediate use of these points, one can assign different dynamics to these points to compress or expand the coverage area.

The major contributions of this brief can be summarized as follows:

1) providing a locally optimum coverage while taking into account the boundary dynamics;
2) providing blanket coverage by moving the coverage region within the boundaries via imposing dynamics on the guidance points;
3) providing coverage control for long regions and passages;
4) changing the coverage area, if necessary, by expanding or compressing the covered region.

The remainder of this brief is structured as follows. Definitions and the problem statement are provided for the blanket coverage control for a long region in Section II. Section III introduces a new approach for optimal Voronoi partitioning and controller design for blanket coverage control. Section IV presents the numerical simulation results to illustrate the optimal coverage for the underlying blanket coverage problem.

A. Notations

We use $\mathbb{N}$, $\mathbb{R}$, and $\mathbb{R}_+$ to, respectively, denote the sets of natural, real, and nonnegative real numbers. Throughout this brief, I_r denotes $r \times r$ identity matrix. We define $\mathcal{Q}$ as a polytope in $\mathbb{R}^2$ and let $\mathcal{Q} = \{Q_1, Q_2, \ldots, Q_t\}$ be a *partition* of $\mathcal{Q}$ as a collection of t closed subsets with disjoint interiors. The boundary of $\mathcal{Q}$ is denoted by $\partial\mathcal{Q}$. Moreover, the so-called *importance* (or *priority*) function is denoted by φ where $\varphi : \mathcal{Q} \to \mathbb{R}_+$ represents the likelihood of an event occurring over the space $\mathcal{Q}$. The function φ is assumed to be measurable and absolutely continuous. The Euclidean distance function is denoted by $\|\cdot\|$, and $|\mathcal{Q}|$ represents the Lebesgue measure of the convex subset $\mathcal{Q}$. The vector set $\mathcal{P} = (p_1, p_2, \ldots, p_n)$ is the location of n agents.

II. Underlying Optimization Problem

In the coverage control literature, the *locational cost function* is defined as a measure of the sensing performance. In this brief, we present a modified version of the locational function that is suitable for the proposed coverage method for n number of agents belonging to P, which is the set of all agents. Assuming that the ith agent is assigned to the region $\mathcal{W}_i$, the objective is to minimize the sensing cost function by finding the optimal locations of the agents and their assigned regions $\mathcal{W}_i$ whose union is $\mathcal{Q}$. In the coverage framework, it is desired to keep the sensing performance as high as possible, while the region associated with agent is changing due to the changing boundaries of the main region. The sensing performance is evaluated as a function of distance from the agent, which needs to be maximized. To this end, we define a sensing cost $f(\|q - p_i\|)$, where $q \in \mathcal{Q}$. The minimization of the sensing cost translates to the maximization of the sensing performance. In this context, the density function is set to be constant to represent the uniform coverage, and all the agents are assigned over the moving space along the given area. A *dynamic partitioning* approach is introduced in this brief to address coverage problems in long regions, such as passages and rivers, where the agents need to move along the boundaries of the blanket to perform the desired coverage task.

A. Voronoi Partitions

The main objective of this brief is to adopt a dynamic coverage approach within the agents deployment and partitioning framework. To achieve this, we need to define an optimization problem that accounts for the changing boundaries of the associated region in a way that it ensures the optimal coverage for a group of moving agents. This optimization problem should consider the individual cost functions defined within the dynamic boundaries of the region associated with all the agents. We first define the collective position of the group of agents through the centroid l as a function of the agents position, i.e., $l = g(p_1, p_2, \ldots, p_n)$. The dependence of l on the position of the agents is discussed later. Next, we partition the changing polytope $\mathcal{Q}$ into a set of Voronoi cells $\mathcal{V}_t(\mathcal{P}) = \{V_1, V_2, \ldots, V_n\}$ generated by the agents $(p_1, p_2, \ldots, p_n)$ as

$$V_m = \{q \in \mathcal{Q} |\ \|q - p_m\| \leq \|q - p_r\|, r = 1, \ldots, n, r \neq m\} \tag{1}$$

where p_m denotes the location of mth agent for $m \in \{1, \ldots, n\}$.

Depending on the position of the agents, they might require a different set of data, i.e., their neighbors' position, to be maintained. Some agents share boundaries only with other agents, while the agents on the boundaries of the region are neighbors not only with other agents but they may also share edges with the polytope $\mathcal{Q}$. In general, the edges associated with each agent ∂V_m are either an edge shared with other agents or edges shared with the dynamic region of the group of agents depending on the position of the agent. An edge that is shared with the neighboring agent f is shown by $\partial V_{m,f}$. The edges associated with the agents on the boundaries that are shared with the main polytope $\mathcal{Q}$, the boundaries of the rear and front lines confining the region are represented by ∂V_m^B, ∂V_m^F, and ∂V_m^R, respectively. Also, ∂V_1^B and ∂V_2^B indicate

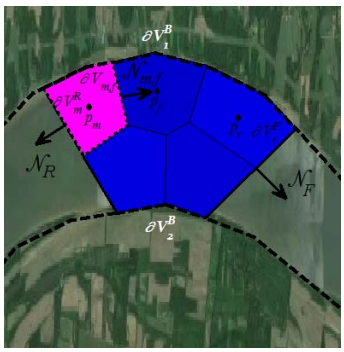

Fig. 1. Illustrative example of the Voronoi partitioning in the blanket coverage of a long region, where the boundaries and their associated normal vectors for the Voronoi cell V_m are shown for the edges shared with fth agent, in addition to the edge ∂V_m^B shared with the main region $\mathcal{Q}$.

the fixed boundaries of the region shown by smooth splines forming the main region that can be a corridor, river, or a passage. Fig. 1 shows the boundaries and their normal vectors for Voronoi cell V_m. We recall the basic characteristics of the Voronoi partitions, including their associated mass, centroid, and polar moment of inertia defined as [21]

$$M_{V_m} = \int_{V_m} \varphi(q)dq, \quad C_{V_m} = \frac{1}{M_{V_m}} \int_{V_m} q\ \varphi(q)dq$$
$$J_{V_m,p_m} = \int_{V_m} \|q - p_m\|^2 \varphi(q)dq. \tag{2}$$

The collective centroid of the agents that is a function of their positions is defined as

$$l = \frac{\sum_{m=1}^{n} M_{V_m} p_m}{\sum_{m=1}^{n} M_{V_m}}. \tag{3}$$

As described earlier, the centroid l is a representative of the collective position of the agents in the blanket that is needed for the computation of the dynamic boundaries of the region $\mathcal{Q}$.

B. Formulation of the Local Optimization Problem

The deployment task in the proposed blanket coverage framework can be addressed by solving an optimization problem over the polytope $\mathcal{Q}$, where the agents position in the region needs to be optimized in the sense of the associated sensing function. Hence, the following cost function is considered:

$$\mathcal{G}(\mathcal{P}, \mathcal{Q}) = \int_{Q_R} \|q - p_R\|^2 \varphi(q)dq + \sum_{m=1}^{n} \int_{Q_m} \|q - p_m\|^2 \varphi(q)dq + \int_{Q_F} \|q - p_F\|^2 \varphi(q)dq \tag{4}$$

where $\mathcal{G}$ is the collective cost function associated with the sensing performance of the agents in the set $\mathcal{P}$. Also, p_F and p_R represent the front and rear guidance points, respectively. The sensing cost is considered as $f(\|q - p_m\|) = \|q - p_m\|^2$ for the mth agent. The solution to (4) gives a local minimum to the deployment problem where agents are considered as the members of a collaborating team sweeping through the region. We define a set of polygons as $\mathcal{Q} = \{Q_1, Q_2, \ldots, Q_n\}$, with disjoint interiors, whose union is $\mathcal{Q}$.

Remark 1: It is proven that among different partitioning schemes, the Voronoi partitions are optimum in the sense of minimizing the defined cost function (4) [21], [22]. Hence, for a given set of agents with position $\mathcal{P} \in \mathcal{Q}$ and a *partition* $\mathcal{Q}$ of $\mathcal{Q}$, we have

$$\mathcal{G}(\mathcal{P}, \mathcal{V}(\mathcal{P})) \leq \mathcal{G}(\mathcal{P}, \mathcal{Q}) \tag{5}$$

which implies that the Voronoi cells represent the optimum partitioning of the area associated with dynamic region of the agents.

We first need to define the dynamic boundaries of the region $\mathcal{Q}$. For this purpose, two virtual points l_R and l_F called guidance points are assigned in the rear and front of the group of agents, respectively. The locations of these points are assumed to be on the trajectory representing the mean of the fixed side boundaries of the main region that is obtained by $\partial V^a = [(\partial V_1^B + \partial V_2^B)/2]$. In other words, these points always have the same distance from the fixed boundaries. The lines representing the dynamic boundaries of the region that confine the coverage area are described by

$$(\mathcal{N}_i)^\top \left(q - \frac{l + p_i}{2}\right) = 0, \quad q \in \partial V_r^i \tag{6}$$

where $i \in \{F, R\}$ and the normal vector $\mathcal{N}_i$ associated with ∂V_r^i is obtained by

$$\mathcal{N}_i = \frac{p_i - l}{\|p_i - l\|}. \tag{7}$$

Equation (6) represents the line drawn between the nucleus of the team of agents and the guidance points (P_R and P_F). As described earlier, the line is changing due to the varying position of the nucleus and guidance points that is translated to dynamic boundaries.

III. Optimal Voronoi Partitioning and Controller Design

The dynamics on the guidance points dictate the speed and direction in which the sensing coverage is carried out on the given area. The next step is to obtain (locally optimum) location of the agents. The derivative of the cost function (4) associated with n agents is

$$\frac{\partial \mathcal{G}}{\partial p_m} = \frac{\partial}{\partial p_m} \left(\int_{Q_R} \|q - p_R\|^2 \varphi(q)dq + \sum_{r=1}^{n} \int_{Q_r} \|q - p_r\|^2 \varphi(q)dq + \int_{Q_F} \|q - p_F\|^2 \varphi(q)dq \right), \quad m = 1, \ldots, n. \tag{8}$$

The solution to this optimization problem differs from that to the conventional sensing cost functions due to the previously defined dependence of the edges of the agents shared with

the boundaries on imposed dynamics of the guidance points. The derivative with respect to the coordinate of agent p_m is obtained as

$$\begin{aligned}\frac{\partial \mathcal{G}}{\partial p_m} = &\int_{V_m} \frac{\partial}{\partial p_m}\|q-p_m\|^2\varphi(q)dq \\ &+\left(\sum_{r=1}^{n}\int_{\partial V_r}\|q-p_r\|^2\varphi(q)\frac{\partial \partial V_r}{\partial p_m}\mathcal{N}_r dq\right. \\ &+\int_{\partial V^F}\|q-p_F\|^2\varphi(q)\frac{\partial \partial V^F}{\partial p_m}\mathcal{N}_F dq \\ &\left.+\int_{\partial V^R}\|q-p_R\|^2\varphi(q)\frac{\partial \partial V^R}{\partial p_m}\mathcal{N}_R dq\right) \end{aligned} \tag{9}$$

where $\partial V^F = \partial \mathcal{Q} \cap \partial \mathcal{Q}_F$ and $\partial V^R = \partial \mathcal{Q} \cap \partial \mathcal{Q}_R$. It can be inferred from the proposed partitioning that the boundaries of the Voronoi cell V_r are either directly or indirectly dependent on p_m. The direct dependence is obviously resulted from the definition of the Voronoi cells (1). We note that V_m and the Voronoi cells in its neighborhood are directly dependent on p_m. The indirect dependence can be seen in the shared boundaries with the guidance agents, where they share at least one edge with the guidance agents (or contribute at least one edge to the boundary of the group of agents).

Remark 2: The integral on each boundary shared with the neighboring agents is identical for agents on both sides except that the normals will have the opposite signs, i.e., $\mathcal{N}_{m,f} = -\mathcal{N}_{f,m}$. Hence, we have

$$\begin{aligned}&\sum_{f\in\mathcal{F}}\int_{\partial V_{m,f}}\|q-p_m\|^2\varphi(q)\frac{\partial \partial V_{m,f}}{\partial p_m}\mathcal{N}_{m,f}dq \\ &\quad = -\sum_{f\in\mathcal{F}}\int_{\partial V_{f,m}}\|q-p_r\|^2\varphi(q)\frac{\partial \partial V_{f,m}}{\partial p_m}\mathcal{N}_{f,m}dq \end{aligned} \tag{10}$$

where $\mathcal{N}_{f,m}$ is the normal vector associated with the edge $\partial V_{f,m}$, and $\mathcal{F} = \{f \,|\, p_f \in \mathcal{N}_{p_m}\}$ with $\mathcal{N}_{p_m}$ representing the set of agents that share boundaries with agent p_m. According to Remark 2, the terms associated with shared boundaries with other neighboring agents will cancel out, and we have

$$\begin{aligned}\frac{\partial \mathcal{G}}{\partial p_m} = &\int_{V_m} \frac{\partial}{\partial p_m}\|q-p_m\|^2\varphi(q)dq \\ &+\left(\sum_{r=1,i\in\{F,R\}}^{n_b}\int_{\partial V_r^i}\|q-p_r\|^2\varphi(q)\frac{\partial \partial V_r^i}{\partial p_m}\mathcal{N}_i dq\right. \\ &+\int_{\partial V^F}\|q-p_F\|^2\varphi(q)\frac{\partial \partial V^F}{\partial p_m}\mathcal{N}_F dq \\ &\left.+\int_{\partial V^R}\|q-p_R\|^2\varphi(q)\frac{\partial \partial V^R}{\partial p_m}\mathcal{N}_R dq\right) \end{aligned} \tag{11}$$

where n_b is the number of agents sharing edges with ∂Q_F and ∂Q_R. Next, to calculate the derivative terms appearing because of the dependence of the shared edges with dynamic boundaries on the nucleus, the chain rule can be applied as follows:

$$\frac{\partial \partial V_r^i}{\partial p_m} = \frac{\partial l}{\partial p_m}\frac{\partial \partial V_r^i}{\partial l} \tag{12}$$

where using (3) and (12), we obtain

$$\frac{\partial}{\partial p_m}\left(l\int_{\mathcal{Q}}\varphi(q)dq\right) = \frac{\partial}{\partial p_m}\left(\sum_{r=1}^{n} p_r\int_{V_r}\varphi(q)dq\right) \tag{13}$$

$$\begin{aligned}&\frac{\partial l}{\partial p_m}\left(\left(\int_{\mathcal{Q}}\varphi(q)dq\right)I_2+\left(\sum_{i\in\{F,R\}}\int_{\partial\mathcal{Q}}\varphi(q)\frac{\partial \partial V^i}{\partial l}\mathcal{N}_i dq\right)l^\top\right) \\ &= \left(\int_{V_m}\varphi(q)dq\right)I_2+\sum_{r=1}^{n}\left(\int_{\partial V_r}\varphi(q)\frac{\partial \partial V_r}{\partial p_m}\mathcal{N}_r dq\right)p_r^\top. \end{aligned} \tag{14}$$

The last term can be discussed in two groups of edges: the ones shared with neighboring agents and the shared edges with dynamic boundaries. It should be noted that only the Voronoi cells associated with the agent located at p_m and its neighbors are dependent on p_m. From (14) and using the chain rule, we obtain

$$\begin{aligned}&\frac{\partial l}{\partial p_m}\left(\left(\int_{\mathcal{Q}}\varphi(q)dq\right)I_2+\left(\sum_{i\in\{F,R\}}\int_{\partial\mathcal{Q}}\varphi(q)\frac{\partial \partial V^i}{\partial l}\mathcal{N}_i dq\right)l^\top\right. \\ &\qquad\left.-\sum_{r=1,i\in\{F,R\}}^{n_b}\left(\int_{\partial V_r^i}\varphi(q)\frac{\partial \partial V_r^i}{\partial l}\mathcal{N}_i dq\right)p_r^\top\right) \\ &= \left(\int_{V_m}\varphi(q)dq\right)I_2+\sum_{p_r\in\{p_m,\mathcal{N}_{p_m}\}}\left(\int_{\partial V_r}\varphi(q)\frac{\partial \partial V_r}{\partial p_m}\mathcal{N}_r dq\right)p_r^\top. \end{aligned} \tag{15}$$

The effect of the moving boundaries with respect to the variation of the centroid of the group of agents is shown by the following notations:

$$M^i_{\partial V_r} = \int_{\partial V_r^i}\varphi(q)\frac{\partial \partial V_r^i}{\partial l}\mathcal{N}_i dq \tag{16}$$

$$M_{\partial\mathcal{Q}} = \sum_{r=1,i\in\{F,R\}}^{n_b} M^i_{\partial V_r} \tag{17}$$

and the changing boundary of the interior agents due to the agents dynamics is represented by

$$M_{\partial V_r} = \int_{\partial V_r}\varphi(q)\frac{\partial \partial V_r}{\partial p_m}\mathcal{N}_r dq. \tag{18}$$

Using these notations results in the following:

$$\begin{aligned}\frac{\partial l}{\partial p_m} = &\left(M_{V_m}I_2+\sum_{p_r\in\{p_m,\mathcal{N}_{p_m}\}}M_{\partial V_r}p_r^\top\right) \\ &\times\left(M_{\mathcal{Q}}I_2+M_{\partial\mathcal{Q}}l^\top-\sum_{r=1,i\in\{F,R\}}^{n_b}M^i_{\partial V_r}p_r^\top\right)^{-1}. \end{aligned} \tag{19}$$

The partial derivative of (6) with respect to l is obtained as

$$\frac{\partial \mathcal{N}_i}{\partial l}\left(q-\frac{p_i+l}{2}\right)+\left(\frac{\partial \partial V_s^i}{\partial l}-\frac{1}{2}\right)\mathcal{N}^i = 0 \tag{20}$$

where

$$\frac{\partial \mathcal{N}_i}{\partial l} = \frac{\mathcal{N}_i(\mathcal{N}_i)^\top - I_2}{\|p_i - l\|}. \tag{21}$$

Substituting (21) into (20), we have

$$\frac{\partial \partial V_s^i}{\partial l}\mathcal{N}_i = \frac{\mathcal{N}_i(\mathcal{N}_i)^\top - I_2}{\|p_i - l\|}\left(\frac{p_i + l}{2} - q\right) + \frac{1}{2}\mathcal{N}_i, \quad q \in \partial V_s^i. \tag{22}$$

Because of the following equality that holds for the variation of the boundary edge ∂V_r^i with respect to the variation of the nucleus l:

$$\frac{\partial \partial V_r^i}{\partial l}\mathcal{N}_i = \frac{\partial \partial V^i}{\partial l}\mathcal{N}_i \tag{23}$$

the derivative (9) can be rewritten as

$$\begin{aligned}\frac{\partial \mathcal{G}}{\partial p_m} &= \int_{V_m} \frac{\partial}{\partial p_m}\|q - p_m\|^2\varphi(q)dq \\ &\quad + \sum_{r=1,i\in\{F,R\}}^{n_b}\int_{\partial V_r^i}\|q - p_r\|^2\varphi(q)\frac{\partial l}{\partial p_m}\frac{\partial \partial V_r^i}{\partial l}\mathcal{N}_i dq \\ &\quad + \int_{\partial V^F}\|q - p_F\|^2\varphi(q)\frac{\partial \partial V^F}{\partial p_m}\mathcal{N}_F dq \\ &\quad + \int_{\partial V^R}\|q - p_R\|^2\varphi(q)\frac{\partial \partial V^R}{\partial p_m}\mathcal{N}_R dq.\end{aligned} \tag{24}$$

Substituting (22) into (24) and using (23), we have

$$\begin{aligned}&\frac{\partial \mathcal{G}}{\partial p_m} \\ &= -2\int_{V_m}(q - p_{sm})\varphi(q)dq + \frac{\partial l}{\partial p_m} \\ &\quad \times\left(\sum_{r=1,i\in\{F,R\}}^{n_b}\left(\frac{\mathcal{N}_i(\mathcal{N}_i)^\top - I_2}{\|l - p_i\|}\int_{\partial V_r^i}\|q - p_r\|^2\varphi(q)\right.\right. \\ &\qquad \left.\times\left(\frac{p_i + l}{2} - q\right)dq + \frac{1}{2}\mathcal{N}_i\int_{\partial V_r^i}\|q - p_r\|^2\varphi(q)dq\right) \\ &\quad + \sum_{i\in\{F,R\}}\left(\frac{\mathcal{N}_i(\mathcal{N}_i)^\top - I_2}{\|l - p_i\|}\int_{\partial V^i}\|q - p_i\|^2\varphi(q)\left(\frac{p_i + l}{2} - q\right)dq\right. \\ &\qquad \left.\left. + \frac{1}{2}\mathcal{N}_i\int_{\partial V^i}\|q - p_i\|^2\varphi(q)dq\right)\right).\end{aligned} \tag{25}$$

Further simplification of (25) using equations of mass and centroid (2) results in

$$\begin{aligned}&\frac{\partial \mathcal{G}}{\partial p_m} \\ &= -2M_{V_m}(C_{V_m} - p_m) \\ &\quad + \left(M_{V_m}I_2 + \sum_{p_r\in\{p_m,\mathcal{N}_{p_m}\}} M_{\partial V_r}p_r^\top\right) \\ &\quad \times\left(M_Q I_2 + M_{\partial Q}l^\top - \sum_{r=1,i\in\{F,R\}}^{n_b} M_{\partial V_r}^i p_r^\top\right)^{-1} \\ &\quad \times\left(\sum_{r=1,i\in\{F,R\}}^{n_b}\left(\frac{\mathcal{N}_i(\mathcal{N}_i)^\top - I_2}{\|l - p_i\|}\int_{\partial V_r^i}\|q - p_r\|^2\varphi(q)\right.\right. \\ &\qquad \left.\left.\times\left(\frac{p_i + l}{2} - q\right)dq + \frac{1}{2}\mathcal{N}_i\int_{\partial V_r^i}\|q - p_r\|^2\varphi(q)dq\right)\right. \\ &\quad + \sum_{i\in\{F,R\}}\left(\frac{\mathcal{N}_i(\mathcal{N}_i)^\top - I_2}{\|l - p_i\|}\int_{\partial V^i}\|q - p_i\|^2\varphi(q)\right. \\ &\qquad \left.\left.\times\left(\frac{p_i + l}{2} - q\right)dq + \frac{1}{2}\mathcal{N}_i\int_{\partial V^i}\|q - p_i\|^2\varphi(q)dq\right)\right).\end{aligned} \tag{26}$$

As the agents move, the change in their position affects the collective centroid l and the boundaries $\partial\mathcal{Q}$ accordingly. This represents the expected sensitivity of the boundaries of the region $\mathcal{Q}$ on the position of p_m. The integral on the boundaries of $\mathcal{Q}$ is calculated once for all the agents at each time step and is applied to obtain the derivative of the cost function associated with different agents.

A. Computation of the Voronoi Cells

The Voronoi cells associated with each agent may require a different set of information to be computed on line. As described before, the agents with edges shared only with other agents are able to compute the Voronoi cell by communicating with the neighboring agents within their group. However, the agents with edges shared with the boundaries ∂Q need the position of the collective centroid of the group, as well as the position of the guidance points p_R and p_F that are known *a priori*. We can implement two alternative communication algorithms; first, it is assumed that all agents communicate with each other meaning that each agent has the location of the other agents. Even though this is not an efficient approach, it can be applied for a small number of agents that are in a relatively close neighborhood of other agents due to the nature of the coverage problems in long narrow regions. These assumptions are realistic due to the fact that the width of the coverage area is limited by the boundaries of the region and the length of the area can be controlled by the relative distance of p_F and p_R.

In an alternative and more efficient communication approach, a greedy algorithm that provides the required data flow within the team and between the so-called leaders of different teams has been proposed in our recent work [22]. To ensure the required data flow, the position of the collective centroid of the group of agents is communicated. This can be implemented when there is a large number of agents covering a large area in some special cases.

B. Controller Design

A gradient decent-based control law is proposed here to ensure the optimal coverage in the sense of minimizing the sensing cost function at each time step. The following dynamics are imposed on each agent:

$$\begin{aligned}\dot{p}_m = u_m &= \frac{K_m}{2M_{V_m}}\left(-\frac{\partial \mathcal{G}}{\partial p_m}\right) \\ &= \frac{K_m}{2M_{V_m}}\left(2M_{V_m}(C_{V_m} - p_m) - \gamma_m\right), \quad m = 1, \ldots, n\end{aligned} \tag{27}$$

where K_m is a positive scalar and

$$\begin{aligned}\gamma_m &= \left(M_{V_m} I_2 + \sum_{p_r \in \{p_m, \mathcal{N}_{p_m}\}} M_{\partial V_r} p_r^\top\right) \\ &\times \left(M_Q I_2 + M_{\partial Q} l^\top - \sum_{r=1, i\in\{F,R\}}^{n_b} M^i_{\partial V_r} p_r^\top\right)^{-1} \\ &\times \left(\sum_{r=1, i\in\{F,R\}}^{n_b} \left(\frac{\mathcal{N}_i(\mathcal{N}_i)^\top - I_2}{\|l - p_i\|} \int_{\partial V_r^i} \|q - p_r\|^2 \varphi(q) \right.\right. \\ &\left. \times \left(\frac{p_i + l}{2} - q\right) dq + \frac{1}{2}\mathcal{N}_i \int_{\partial V_r^i} \|q - p_r\|^2 \varphi(q) dq\right) \\ &+ \sum_{i\in\{F,R\}} \left(\frac{\mathcal{N}_i(\mathcal{N}_i)^\top - I_2}{\|l - p_i\|} \int_{\partial V^i} \|q - p_i\|^2 \varphi(q) \right. \\ &\times \left(\frac{p_i + l}{2} - q\right) dq + \frac{1}{2}\mathcal{N}_i \\ &\left.\left. \times \int_{\partial V^i} \|q - p_i\|^2 \varphi(q) dq\right)\right). \end{aligned} \tag{28}$$

By dividing K_m by the varying term $2M_{V_m}$, the control input is normalized to distribute the effect of both $2M_{V_m}(C_{V_m} - p_m)$ and γ_m in the controller design. While the first term drives the agent toward its centroid, the second term is associated with the changing boundaries of the coverage area Q. In other words, the above control law ensures that the agents are confined within the given dynamic boundaries of Q. It should be noted that throughout this brief, the partitions of regions associated with each agent are assumed to be convex or near convex due to the smoothness of the splines defining the boundaries of the river and border regions.

Remark 3: When the centroid of near convex regions falls outside the coverage region, the agents move toward the centroid and each agent finally converges to the closest point to the centroid in its associated coverage area.

Remark 3 follows the same line as in [23], where the nonconvexity in coverage problems is addressed by providing near optimal solutions. Due to the smoothness of the boundaries, the proposed framework of this brief is also expected to provide near optimum configurations. As discussed earlier, the guidance points are required to move along the trajectory representing the mean of the boundaries of the coverage region. This ensures that the blanket area remains inside the main coverage region that is imposed by the defined trajectory ∂V^a of the guidance points. Hence, the following dynamics are imposed on the guidance points:

$$\dot{P}_R = K_R(\partial V^a - P_R), \quad \dot{P}_F = K_F(\partial V^a - P_F) \tag{29}$$

where K_F and K_R are positive scalars. Due to the dynamics of the boundaries of the moving blanket coverage area, the imposed dynamics on the guidance points and the agents have to ensure the convergence to the optimal configuration from the coverage perspective. To this end, the agents need to have faster dynamics than the dynamics imposed on the guidance points that change the boundaries and hence move the region Q along the main region. This is due to the fact that agents should be able to converge to their local optima as the coverage area changes, via the imposed dynamics on the guidance points. This prevents the agents falling behind the changing coverage area and enables them to provide a locally optimum coverage. Regardless of the chosen dynamics, after converging to the first optimal configuration, the next convergence to new optimal configurations is expected to be faster. It is mainly because each optimal configuration is considered as the initial condition for the next configuration associated with the new Q, and hence, the location of the agents is near optimal at each time step associated with the guidance points.

C. Convergence of the Proposed Controller

As described before, the proposed controller provides optimal coverage within the blanket coverage framework by driving the agents to their local optima. The dynamics of the boundaries of the coverage region are taken into account in the proposed control law. It should be noted that throughout this brief, it is assumed that the agents move at faster dynamics than the blankets. This is to ensure that agents can move to their optimal configuration, while blanket is sliding through the boundaries of the region. Given the aforementioned assumptions and to show the convergence of the agents to their collective local optimum, the following lemma is provided.

Lemma 1: The agents converge to a local minimum to maximize the sensing performance by imposing the proposed control law given in (27). That is

$$\lim_{\tau\to\infty} \| - 2M_{V_m}(\tau)(C_{V_m}(\tau) - p_m(\tau)) + \gamma_m(\tau)\| = 0 \tag{30}$$

for $\forall m \in \{1, \ldots, n\}$.

Proof: The asymptotic behavior cannot be proven by invoking standard invariant set theorems for time-varying systems. We hence use Barbalat's lemma to prove the asymptotic convergence of the system when the agents traverse to their local optimum. To this aim, the following Lyapunov-like function associated with each agent is defined:

$$V = \mathcal{G}. \tag{31}$$

The derivative of this function is obtained as

$$\dot{V} = \sum_{m=1}^{n} \left(\frac{\partial p_m}{\partial \tau}\right)^\top \frac{\partial \mathcal{G}}{\partial p_m}. \tag{32}$$

Substituting (26) and (27) into (32), we obtain

$$\begin{aligned}\dot{V} = -\sum_{m=1}^{n} \frac{K_m}{2M_{V_m}} &\left(-2M_{V_m}(C_{V_m} - p_m) + \gamma_m\right)^\top \\ &\times \left(-2M_{V_m}(C_{V_m} - p_m) + \gamma_m\right). \end{aligned} \tag{33}$$

Since M_{V_m} and K_m are positive scalars, it can be concluded that the derivative (32) is nonpositive, $\dot{V} \leq 0$. Due to the positivity of the cost function $\mathcal{G}$, it is also concluded that the Lyapunov-like function (31) is nonincreasing and hence lower bounded. As shown in [24], $\ddot{V}(\tau)$ is uniformly bounded that

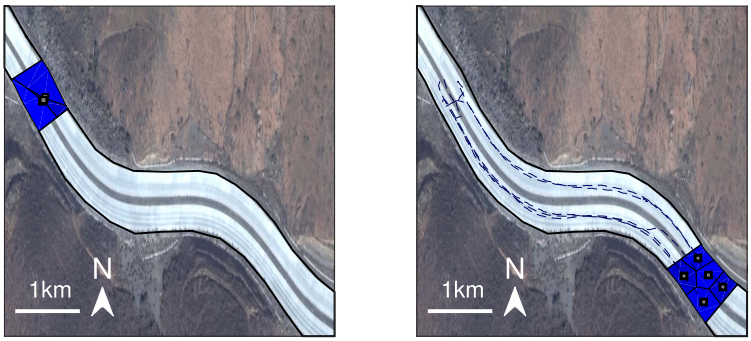

Fig. 2. Initial (left) and final (right) configurations for a group of five agents maintaining the desired coverage throughout the illustrated section of a border buffer zone. Dashed lines: traversed trajectory by agents.

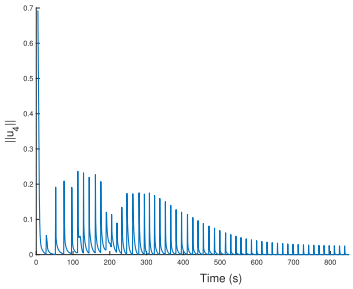

Fig. 3. Control input associated with one of the agents while performing the blanket coverage task.

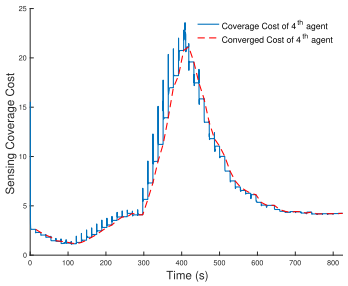

Fig. 4. Coverage cost and final converged cost at each blanket area for one of the agents while moving through the buffer zone.

results in the uniform continuity of $\dot{V}(\tau)$. Next, since $V(\tau)$ is bounded and due to the continuity of $\dot{V}(\tau)$, it is proven by Barbalat's lemma that $\lim_{\tau\to\infty}\dot{V}=0$, and hence, (30) is obtained. ■

IV. Simulation Results and Discussion

The proposed blanket coverage method of this brief is evaluated using numerical examples that investigate its capability in providing an optimal coverage in rivers. As the first example, a section of a border area is chosen to deploy a group of monitoring agents along the buffer zone. Five agents are deployed to move along the buffer zone and gather the required information while maintaining the desired optimum coverage at each portion of the border area. As shown in Fig. 2, the agents converge to a final configuration as the coverage area moves along the defined trajectory for the guidance points. The control input associated with one of the agents in this example is shown in Fig. 3. As observed, at each iteration (blanket), there is a jump in the control signal due to the moving blanket; it is then decreased as agents approach their optimal positions for each blanket area before it moves to the next position. The same pattern is repeated throughout the deployment as agents and the blanket move through the boundaries of the region. The agents dynamics are imposed by choosing $K_m = 0.25$, and also, in this case, $K_R = K_F = 0.18$ that allows for a uniform coverage throughout the region. Fig. 4 shows the coverage cost for the moving blanket throughout the border buffer zone. The coverage cost for each blanket converges to a final value, and the process is repeated as blanket moves through the buffer zone. As observed, the coverage cost is optimized at each blanket area leading to optimal coverage that is illustrated by the converged coverage cost. The cost also converges to a final value as blanket moves toward the endpoint.

To evaluate the proposed approach on a different example, a section of Ohio river is used for the coverage purpose, as shown in Fig. 5. The river is located on the border line of the states of Illinois and Kentucky and is considered to be a wildlife preserve. The given section of the river that is located in a hard-to-access area is chosen to deploy the agents to perform the assigned monitoring task. The results indicate that the agents are capable of moving within the boundaries of the river. The presented results are obtained for $K_m = 0.82$ and we also assign $K_R = K_F = 0.31$. As mentioned before, this approach allows for either expanding or compressing the covered area through changing the relative distance of the guidance points. This can be seen in Fig. 6, where the results are shown for both cases. Due to the nature of the coverage task, it is very likely that a portion of the river requires a more accurate monitoring. The proposed approach provides a flexible tool by assigning a smaller or larger area to each agent to achieve a stronger or more moderate sensory coverage, respectively. The dynamics on the guidance points are imposed by $K_R = 0.26$ and $K_F = 0.16$ and $K_R = 0.22$ and $K_F = 0.33$ for the compression and expansion examples, respectively.

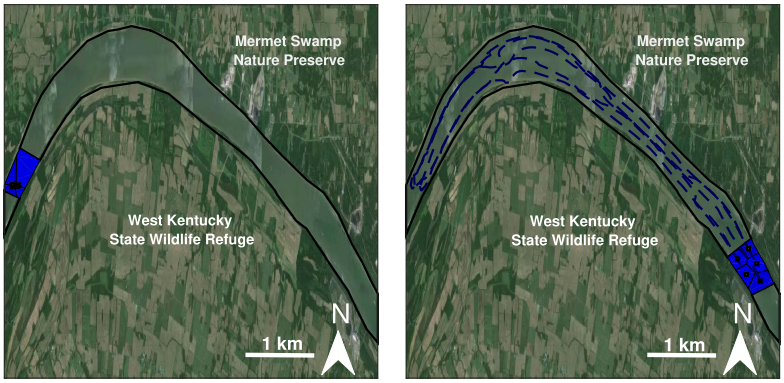

Fig. 5. Initial (left) and final (right) configurations for a group of five agents maintaining optimum coverage throughout a section of the Ohio river. Dashed lines: paths of the agents.

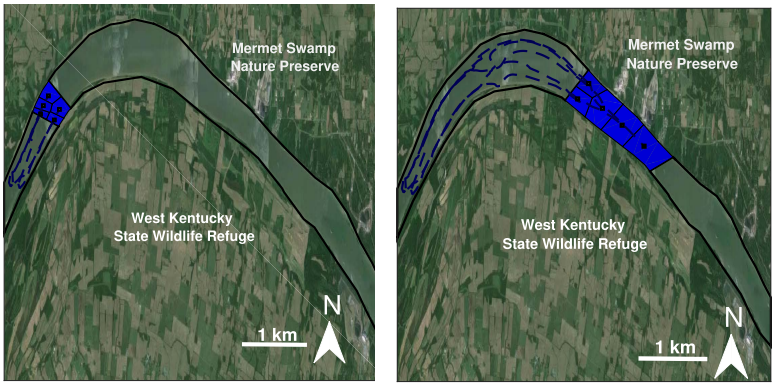

Fig. 6. Illustration of the compressed (left) and expanded (right) configurations for a group of five agents maintaining an optimum coverage. Dashed lines: paths of the agents.

V. Conclusion

To cope with the complexity of the coverage problems in real-world applications, a blanket coverage approach for long regions, such as rivers and border buffer zones, is presented in this brief. The proposed approach ensures the local optimum coverage over the blankets leading to the partitioning of the dynamic region by dividing it into multiple subregions associated with multiple deployed agents. This is beneficial to handle tasks where it is required to cover long regions, such as rivers or border buffer zones. Therefore, as the blanket coverage area moves within the boundaries of the environment, the agents provide optimal coverage for each dynamic region. The developed method also allows for compressing or expanding the blanket coverage area. This is particularly useful when it is required to gather more accurate data in a section of the region, or when a larger area needs to be covered at a different section. In essence, the proposed control law provides the means to monitor long regions and can guarantee the optimum coverage.

References

[1] R. Patel, P. Frasca, J. W. Durham, R. Carli, and F. Bullo, "Dynamic partitioning and coverage control with asynchronous one-to-base-station communication," *IEEE Trans. Control Netw. Syst.*, vol. 3, no. 1, pp. 24–33, Mar. 2016.

[2] J. Habibi, H. Mahboubi, and A. G. Aghdam, "A gradient-based coverage optimization strategy for mobile sensor networks," *IEEE Trans. Control Netw. Syst.*, vol. 4, no. 3, pp. 477–488, Sep. 2017.

[3] M. Garey, D. Johnson, and H. Witsenhausen, "The complexity of the generalized Lloyd-max problem (corresp.)," *IEEE Trans. Inf. Theory*, vol. IT-28, no. 2, pp. 255–256, Mar. 1982.

[4] S. Lloyd, "Least squares quantization in PCM," *IEEE Trans. Inf. Theory*, vol. IT-28, no. 2, pp. 129–137, Mar. 1982.

[5] Y. Ouyang, "Evaluation of river water quality monitoring stations by principal component analysis," *Water Res.*, vol. 39, no. 12, pp. 2621–2635, 2005.

[6] V. Simeonov, J. W. Einax, I. Stanimirova, and J. Kraft, "Environmetric modeling and interpretation of river water monitoring data," *Anal. Bioanal. Chem.*, vol. 374, no. 5, pp. 898–905, 2002.

[7] X. Sun, S. S. Ge, J. Zhang, and X. Cao, "Region tracking control for high-order multi-agent systems in restricted space," *IET Control Theory Appl.*, vol. 10, no. 4, pp. 396–406, 2016.

[8] A. S. Matveev, A. A. Semakova, and A. V. Savkin, "Range-only based circumnavigation of a group of moving targets by a non-holonomic mobile robot," *Automatica*, vol. 65, pp. 76–89, Mar. 2016.

[9] M. Dunbabin and L. Marques, "Robots for environmental monitoring: Significant advancements and applications," *IEEE Robot. Autom. Mag.*, vol. 19, no. 1, pp. 24–39, Mar. 2012.

[10] F. Abbasi, A. Mesbahi, and J. M. Velni, "A team-based approach for coverage control of moving sensor networks," *Automatica*, vol. 18, pp. 342–349, Jul. 2017.

[11] S. Achar, B. Sankaran, S. Nuske, S. Scherer, and S. Singh, "Self-supervised segmentation of river scenes," in *Proc. IEEE Int. Conf. Robot. Autom. (ICRA)*, May 2011, pp. 6227–6232.

[12] S. Nuske *et al.*, "Autonomous exploration and motion planning for an unmanned aerial vehicle navigating rivers," *J. Field Robot.*, vol. 32, no. 8, pp. 1141–1162, 2015.

[13] A. Marino, L. E. Parker, G. Antonelli, and F. Caccavale, "A decentralized architecture for multi-robot systems based on the null-space-behavioral control with application to multi-robot border patrolling," *J. Intell. Robot. Syst.*, vol. 71, nos. 3–4, pp. 423–444, 2013.

[14] M. Dunbabin, A. Grinham, and J. Udy, "An autonomous surface vehicle for water quality monitoring," in *Proc. Austral. Conf. Robot. Autom. (ACRA)*, Dec. 2009, pp. 2–4.

[15] M. Dunbabin and A. Grinham, "Experimental evaluation of an autonomous surface vehicle for water quality and greenhouse gas emission monitoring," in *Proc. IEEE Int. Conf. Robot. Autom. (ICRA)*, May 2010, pp. 5268–5274.

[16] A. S. Matveev, H. Teimoori, and A. V. Savkin, "A method for guidance and control of an autonomous vehicle in problems of border patrolling and obstacle avoidance," *Automatica*, vol. 47, no. 3, pp. 515–524, 2011.

[17] L. DeVries and D. A. Paley, "Multivehicle control in a strong flowfield with application to hurricane sampling," *J. Guid., Control, Dyn.*, vol. 35, no. 3, pp. 794–806, 2012.

[18] S. Minaeian, J. Liu, and Y. J. Son, "Vision-based target detection and localization via a team of cooperative UAV and UGVs," *IEEE Trans. Syst., Man, Cybern., Syst.*, vol. 46, no. 7, pp. 1005–1016, Jul. 2016.

[19] F. Santoso, "Range-only distributed navigation protocol for uniform coverage in wireless sensor networks," *IET Wireless Sensor Syst.*, vol. 5, no. 1, pp. 20–30, 2015.

[20] M. Li, Z. Li, and A. V. Vasilakos, "A survey on topology control in wireless sensor networks: Taxonomy, comparative study, and open issues," *Proc. IEEE*, vol. 101, no. 12, pp. 2538–2557, Dec. 2013.

[21] J. Cortes, S. Martinez, T. Karatas, and F. Bullo, "Coverage control for mobile sensing networks," *IEEE Trans. Robot. Autom.*, vol. 20, no. 2, pp. 243–255, Apr. 2004.

[22] F. Abbasi, A. Mesbahi, and J. Mohammadpour, "Team-based coverage control of moving sensor networks," in *Proc. Amer. Control Conf. (ACC)*, Jul. 2016, pp. 5691–5696.

[23] A. Breitenmoser, M. Schwager, J.-C. Metzger, R. Siegwart, and D. Rus, "Voronoi coverage of non-convex environments with a group of networked robots," in *Proc. IEEE Int. Conf. Robot. Autom. (ICRA)*, May 2010, pp. 4982–4989.

[24] M. Schwager, D. Rus, and J.-J. Slotine, "Decentralized, adaptive coverage control for networked robots," *Int. J. Robot. Res.*, vol. 28, no. 3, pp. 357–375, Mar. 2009.